Quantum dynamical treatment of inelastic scattering of atoms at a surface at finite temperature: The random phase thermal wave function approach

M. Nest[a)]
Institut für Chemie, Universität Potsdam, Karl-Liebknecht-Str. 25, 14476 Potsdam, Germany

R. Kosloff
Department of Physical Chemistry, Hebrew University, Jerusalem 91904, Israel

(Received 1 June 2007; accepted 23 August 2007; published online 5 October 2007)

We present quantum dynamical calculations for the inelastic scattering of atoms at a nonrigid surface at finite temperature. The surface degrees of freedom are discretized and treated in a multiconfigurational wave function picture. The thermal averaging is carried out with the random phase thermal wave function approach. We show that it is sufficient to restrict the random phases to the intermediate basis of single particle functions, discuss the convergence of the method with the number of configurations and realizations, and analyze the flow of energy between different parts of the system for a range of temperatures between 4 and 500 K. © *2007 American Institute of Physics*. [DOI: 10.1063/1.2786088]

I. INTRODUCTION

Quantum systems which interact with an environment are ubiquitous in chemistry and physics.[1,2] This includes, for example, processes such as surface mediated reactions,[3,4] reactions in solution,[5] or systems which are driven by external fields.[6] The environment can serve as an energy sink or as a source of phase fluctuations. Since quantum calculations scale exponentially with the number of degrees of freedom, dynamical simulations require a reduced description where the system is treated explicitly and the environment is treated in a less rigorous level.[1] The prospect of quantum computers, of which the functionality depends sensitively on the absence of external perturbations, has added renewed interest in the decoherence introduced by the environment.[7,8]

The main tool to treat open quantum systems has for many decades been the reduced density operator formalism referred to as system-bath problems. The full Hamiltonian operator is customarily divided into three parts,

$$\hat{H} = \hat{H}_S + \hat{H}_I + \hat{H}_B, \tag{1}$$

where $\hat{H}_S$ describes the system, $\hat{H}_B$ the bath, and $\hat{H}_I$ the system-bath coupling. The next step is to obtain a reduced equation of motion for the system density operator. Some approaches employ a perturbation expansion in $\hat{H}_I$, so that they are valid in the weak coupling limit.[1,2,9–15] An alternative is to impose Markovian conditions, leading to quantum dynamical semigroups.[16] Both derivations lead to a reduced equation of motion for the system density operator,

$$\dot{\hat{\rho}}_s = \mathcal{L}(\hat{\rho}_s) = \frac{i}{\hbar}[\hat{H}_S^n, \hat{\rho}_s] + \mathcal{L}_D(\hat{\rho}_s), \tag{2}$$

where $\hat{\rho}_s$ is the system density operator, $\hat{H}_S^n$ is an effective system Hamiltonian, and $\mathcal{L}_D$ represents the dissipative Liouville operator which implicitly describes the bath influence on the system. Non-Markovian extensions have also been introduced.

The difficulty with the reduced density operator approaches is that except for simple model systems the derivations leading to $\mathcal{L}_D$ are difficult to carry out in a controlled fashion. In particular, when external fields are involved, $\mathcal{L}_D$ is modified,[17] and special care has to be used not to violate the second law of thermodynamics.[18] The reduced density approach naturally can be extended to mixed state finite temperature simulations. Numerical simulations based on solving the equation of motion of the density operator have been used extensively.[19–21]

In recent years, a different approach termed the "surrogate Hamiltonian" has been developed to overcome the difficulties of the reduced density operator approach.[22] In the surrogate Hamiltonian, the bath is discretized and represented by a large number of representative modes which are either harmonic oscillators or two-level systems. As the number of bath modes increases, the description converges. The two types of bath modes—harmonic and spin baths—represent two generic limits.[23] For the harmonic bath the system-bath coupling can be encoded into the spectral density function. Effective simulation methods have been derived to calculate this function. In some cases, the spin bath can be mapped to the harmonic bath,[24] so the same input can be used to model the bath.

The usefulness of the surrogate Hamiltonian method depends on the ability to propagate in time very large wave functions. It seems natural to restrict the degree of quantum

[a)]Author to whom correspondence should be addressed. Electronic mail: mnest@uni-potsdam.de

correlations between the bath degrees of freedom. The multiconfiguration time-dependent Hartree[25–27] (MCTDH) method does just that. With this method the combined wave functions with up to about 100 degrees of freedom (DoF) can be simulated. Modifications of MCTDH, such as mutlilayer MCTDH (Refs. 28 and 29) and the local coherent state approximation,[30] can treat several thousand DoFs, in system-bath type situations. Obviously, the propagation of a wave function is an exact representation of a bath only if the bath/environment is at 0 K temperature.

The purpose of the present paper is to overcome this flaw so that the applicability of the MCTDH method is extended to finite temperatures. The basic idea is to construct the finite temperature density operator from a stochastic average of several properly chosen wave functions. Stochastic sampling of the Boltzmann operator has already been done for a variety of problems. Wang and Thoss used an importance sampling Monte-Carlo technique, in order to calculate thermal correlation functions.[29] Manthe *et al.* have employed a random phase scheme similar to ours in the calculation of partition functions and rate constants of gas phase reactions.[31,32] They are using the MCTDH method for the propagation, too, but apply the random phases on the level of the single particle functions, instead of the Hartree products, as in this work. Also, while Manthe *et al.* treated thermal systems, we are treating thermal baths. finally, the random phase thermal wave function method has also been used to study the dissipating effect of spin baths.[33] Random phase thermal wave functions have Boltzmann weighted amplitudes in the energy representation and random phase. Averaging different realization of the random phase is equivalent to a thermal density operator. It was shown that the number of realizations required to achieve convergence becomes very small when the size of the Hilbert space is large.

In this paper, we will adapt the random phase thermal wave function[33] to the work with the intermediate basis of Hartree products of the MCTDH method. As a model application we have chosen the inelastic scattering of an atom at a nonrigid surface at finite temperature. This process describes an elementary step in various reactions, such as heterogeneous catalysis and molecular hydrogen formation in interstellar space. The same process has already been investigated in various other studies of discretized baths[34,35] and open system quantum dynamics.[36]

In Sec. II, we start with a description of the physical system that we want to study and specify the Hamiltonian of the system, the coupling, and the bath. Next, this will be used to explain how the random phase thermal wave function approach can treat thermal ensembles within a wave function picture. At the end of Sec. II, we describe briefly the MCTDH method, which is an essential tool, when wave functions of very high dimensionality are to be treated. In Sec. III, we apply this approach to the problem of inelastic scattering and sticking of an atom from a platinum surface at finite temperature. Atomic units will be used throughout this paper, if not stated otherwise.

II. THEORY

A. The model

The Hamiltonian [Eq. (1)] for a surface encounter consists of three parts, describing the system (scattering atom), the bath (surface), and the interaction between the two. The system Hamiltonian contains the kinetic energy and the Born-Oppenheimer potential energy surface (PES) along a single coordinate z (the atom-surface distance) for the scatterer,

$$\hat{H}_s = \frac{\hat{p}^2}{2M} + \hat{V}(z). \tag{3}$$

For the mass M we take $25\,000 m_e$, which is representative for light atoms. From a chemical point of view, the PES is part of the *interaction* with the surface, but traditionally, this is included in $\hat{H}_s$ because $\hat{V}(z)$ does not depend on bath degrees of freedom. However, the dependences of $\hat{H}_s$ and $\hat{H}_I$ on z should be similar. For the potential $\hat{V}(z)$ describing the atom-surface interaction we choose a Morse function,

$$\hat{V}(z) = D(e^{-2\alpha z} - 2e^{-\alpha z}), \tag{4}$$

with a well depth $D=0.5$ eV and $\alpha=2a_0^{-1}$. These values, as well as those that follow below, are chosen to be representative for physisorption of a light atom on a single crystal surface. From the Morse parameters D and α above we find a harmonic frequency around the potential minimum of $\omega_M = 0.002\,425 E_h/\hbar$.

The bath is represented by a set of N Harmonic oscillators,

$$\hat{H}_B = \sum_{k=1}^{N} \frac{\hat{p}_k^2}{2m} + \frac{m\omega_k^2}{2}\hat{q}_k^2. \tag{5}$$

In our application in Sec. III, we will set $N=20$, so that the full wave function is 21 dimensional. For simplicity we choose bath oscillators with equidistant frequencies, $\omega_k = k\Delta\omega$, and the highest frequency of the bath is set to $N\Delta\omega = 0.005 E_h/\hbar$. The consequences of this choice will be discussed in Sec. III. The interaction Hamiltonian is linear in the bath coordinates and nonlinear in z. This is to ensure that the rate of energy dissipation vanishes far from the surface,

$$\hat{H}_I = -\sum_{k=1}^{N} c_k \frac{1 - e^{-\alpha z}}{\alpha}\hat{q}_k. \tag{6}$$

A frequency independent, Ohmic damping is achieved for coupling coefficients,

$$c_k = \left(\frac{2mM\gamma\Delta\omega^3}{\pi}\right)^{1/2} k. \tag{7}$$

It should be noted that both the bath and the interaction Hamiltonian are effectively independent of the mass m, which can be seen by the substitutions,

$$\hat{q}_k \to \frac{1}{\sqrt{m\omega_k}}\hat{Q}_k, \quad \hat{p}_k \to \sqrt{m\omega_k}\hat{P}_k. \tag{8}$$

The parameters γ has the unit of rate and scales the overall coupling strength. We choose $\gamma = 1/(1\ \text{ps})$, which is a typical vibrational lifetime of adsorbed atoms.

B. Random phase thermal wave functions

The random phase thermal wave function technique is a stochastic approach to evaluate the Boltzmann operator. A general thermal state is described by the density operator,

$$\hat{\rho}(\beta) = \frac{e^{-\beta\hat{H}_0}}{Z}, \tag{9}$$

with the inverse temperature $\beta = 1/(k_B T)$ and the partition function $Z = \mathrm{Tr}\{e^{-\beta\hat{H}_0}\}$. For the gas surface encounter the initial state is a direct product of a thermal bath and a pure state describing the incident scatterer far from the surface. The relevant bath Hamiltonian for Eq. (9) is therefore

$$\hat{H}_0 = \sum_{k=1}^{N} \frac{\hat{p}_k^2}{2m} + \frac{m\omega_k^2}{2}\hat{q}_k^2 - \frac{c_k}{\alpha}\hat{q}_k. \tag{10}$$

Despite the shift $c_k\hat{q}_k/\alpha$, the bath is still harmonic, and the eigenvalues and eigenfunctions are analytically known. However, this does not lead to a practical sampling scheme for the Boltzmann operator. Even if on average only two states per degree of freedom were occupied, then this would result already in more than 1×10^6 states for the full bath.

The random phase thermal wave function approach offers a different route to solve this problem. In the following, we will outline the general idea and discuss the modifications for multiconfigurational wave functions in Sec. II C. Let us assume that we have a complete basis $\{\phi_l\}$ to represent states of the bath described by $\hat{H}_0$. From this, we can construct "infinite temperature" wave functions with random phases according to

$$|\Phi(\boldsymbol{\theta})\rangle = \frac{1}{\sqrt{L}}\sum_{l=1}^{L} e^{i\theta_l}|\phi_l\rangle, \tag{11}$$

where $\boldsymbol{\theta}$ is a vector of random phases, $|\phi_l\rangle$ is a complete basis, and L is the size of the Hilbert space. Next, we note that the identity operator $\hat{I}$ can be written as a sum over projectors on these random phase wave functions,

$$\hat{I} = \lim_{K\to\infty} \frac{1}{K}\sum_{k=1}^{K} |\Phi(\boldsymbol{\theta}_k)\rangle\langle\Phi(\boldsymbol{\theta}_k)|. \tag{12}$$

Inserting this into the definition of the Boltzmann operator [Eq. (9)] gives

$$\hat{\rho}(\beta) = \frac{1}{Z}e^{-(\beta/2)\hat{H}_0}\hat{I}e^{-(\beta/2)\hat{H}_0}, \tag{13}$$

$$= \lim_{K\to\infty} \frac{1}{Z}\frac{1}{K}\sum_{k=1}^{K} |\Phi(\beta/2,\boldsymbol{\theta}_k)\rangle\langle\Phi(\beta/2,\boldsymbol{\theta}_k)|, \tag{14}$$

where the *random phase thermal wave function* $|\Phi(\beta/2,\boldsymbol{\theta}_k)\rangle$ is obtained by propagation in imaginary time up to $\beta/2$. With this, we have established all that is necessary to calculate thermal expectation values of observables,

$$\langle\hat{A}\rangle = \mathrm{Tr}\{\hat{\rho}\cdot\hat{A}\}, \tag{15}$$

$$= \lim_{K\to\infty} \frac{1}{Z}\frac{1}{K}\sum_{k=1}^{K} \langle\Phi(\beta/2,\boldsymbol{\theta}_k)|A|\Phi(\beta/2,\boldsymbol{\theta}_k)\rangle. \tag{16}$$

This approach, as every statistical sampling scheme, converges as $1/\sqrt{K}$ with the number of realizations. However, the error σ is also a function of the size L of the Hilbert space,

$$\sigma = \frac{\lambda(L)}{\sqrt{K}}. \tag{17}$$

If $\lambda(L)$ is a decreasing function of L, then the random phase thermal wave function approach will become more efficient with system size. In fact, Gelman and Kosloff found such a behavior in Ref. 33.

C. Multiconfiguration time-dependent Hartree

The essentials of the MCTDH approach to quantum dynamics has been previously described.[25–27] It is therefore sufficient to establish the essential equations which are important in the application to the random phase thermal wave function method. In MCTDH, the wave function is expanded into a large number of Hartree products,

$$\Psi(x_1,\ldots,x_f,t) = \sum_{j_1=1}^{n_1}\cdots\sum_{j_f=1}^{n_f} A_{j_1\cdots j_f}(t)\prod_{k=1}^{f}\varphi_{j_k}^{(k)}(x_k,t). \tag{18}$$

Here, we have denoted the number of degrees of freedom by f, which is equal to $N+1$ for the Hamiltonian specified in the previous subsections. The main advantage of MCTDH stems from the fact that the single particle functions (SPF) $\varphi_{j_k}^{(k)}$ are time dependent and form some sort of intermediate basis. They are in turn defined on a time-independent, "primitive" basis $\chi^{(k)}$,

$$\varphi_{j_k}^{(k)}(x_k,t) = \sum_{\alpha=1}^{N_k} d_{j_k\alpha}^{(k)}(t)\chi_\alpha^{(k)}, \tag{19}$$

which can be grid points, eigenstates of a one-dimensional Hamiltonian, etc. The equations of motion can be found, e.g., in Ref. 26. They were solved with the Heidelberg MCTDH program package.[37] It should be noted that we used the so-called variable mean field version, with the corresponding choice of constraint operators, because we obtained converged results already for a much smaller number of SPFs, compared to the constant mean field integration scheme. For the bath modes a mode combination scheme[26,27] has been used, for which we give the parameters in the following section.

III. APPLICATION

The system studied is the gas surface encounter leading to sticking. We first analyze the typical time scales and en-

TABLE I. Standard mode combination scheme for the MCTDH wave function used in this paper. The second column identifies the modes that are combined, i.e., propagated on a product grid. They are ordered from low to high-frequency modes. The third column gives the number of SPFs, and columns from four to six give the maximum over time of the smallest natural population of that mode.

No.	Modes	SPF Nos. ($\tilde{n}_k$)	4 K	300 K	500 K
1	z	8	0.02	0.01	0.01
2	x_1,x_2,x_3,x_4	5	0.00	0.06	0.10
3	x_5,x_6,x_7,x_8	5	0.00	0.05	0.09
4	x_9,x_{10},x_{11},x_{12}	5	0.00	0.02	0.07
5	$x_{13},x_{14},x_{15},x_{16}$	4	0.00	0.02	0.07
6	$x_{17},x_{18},x_{19},x_{20}$	3	0.00	0.01	0.06

ergies involved in the process. A set of harmonic oscillators with equidistant frequencies has a well defined recurrence time of $2\pi/\Delta\omega$, which is for our system equal to 608 fs. This has to be compared with the total duration of the scattering process. We chose an initial momentum of the scattering atom of $p_0=-9.585\hbar/a_0$, so that sticking probabilities can be obtained with 450 fs propagation time, which is well below the recurrence time. The momentum corresponds to an initial kinetic energy of the atom of $E_{\mathrm{kin}}(t=0)=50$ meV$=D/10$. This also sets the interesting temperature range, through the relation $E_{\mathrm{kin}}/k_B=T=580$ K. To be more precise, only a single SPF of the system, for $j_1=1$, is occupied,

$$\varphi_1^{(1)}(z,t=0)=\frac{1}{\sqrt{\sigma\sqrt{\pi}}}e^{-(z-z_0)^2/(2\sigma)^2+ip_0z}, \tag{20}$$

with a center at $t=0$ of $z_0=5a_0$ and a width $\sigma=1a_0$. The remaining seven SPFs with $j_1=2,\ldots,8$ are unoccupied. The second relevant time scale of the bath is the bath response time, given by the surface oscillator with the highest frequency. Its oscillation period of $2\pi/(N\Delta\omega)=30$ fs is short enough for the bath to react almost instantly to the incident atom.

The procedure to calculate a temperature dependent sticking probability with the random phase thermal MCTDH wave function approach [see Eq. (16)] consists of the following steps:

(1) An infinite temperature wave function with random phases is constructed. To this end, the coefficients $A_{1j_2,\ldots,j_6}$ of the combined modes are assigned complex numbers of modulus 1 and random angle. If the first index is different from 1, then the corresponding $A_{j_1,\ldots,j_6}$ are zero because only a single SPF of the subsystem is occupied.

(2) The wave function is then propagated in imaginary time to $\beta/2$. After that, the eigenstates of the bath are populated according to a Boltzmann distribution. (At least in the limit of infinitely many SPFs.) The lower the frequency of a surface oscillator, the higher are the quantum numbers of states with a noticeable occupation at a given temperature. Therefore, these modes have to have a larger number of SPFs, than the high-frequency oscillators (see Table I). The propagation in imaginary time is done with the Hamiltonian $\hat{H}_0$ [see Eq. (10)] so that the system degree of freedom is not affected.

(3) The system is propagated for 450 fs in real time, which takes about 3 h CPU time on a modern personal computer. This is the most time consuming part of the algorithm.

(4) To analyze the results, the reduced density matrix $\rho(z,z',t)$ of the system is calculated, by tracing over all bath modes. The sticking probability is obtained from this, by projection on all bound states of the system Hamiltonian $\hat{H}_S$.

(5) Steps 1–4 are repeated, and the expectation values are incoherently averaged, until convergence is achieved. Typically, we made 60 realizations for each temperature.

One important point that we want to show in this paper is that it is sufficient to apply the random phases to the intermediate basis of single particle functions. The line of reasoning here is as follows: In the limit that the number of SPFs is equal to the number of primitive grid points, $n_k=N_k$, MCTDH is exact. If less SPFs are used, then the Hartree products form some kind of intermediate basis, which restricts the amount of correlation that is actually accounted for. What we have to do, therefore, is to estimate the error due to the limited number of SPFs. Table I gives our standard mode combination scheme and the number of SPFs per mode for our standard configuration. Thus, 1500 random coefficients $A_{1j_2,\ldots,j_6}$ are required per random phase wave function.

Figure 1 illustrates the trapping process, when the temperature of the surface is 300 K. The upper panel shows the sticking probability as a function of time, for a single realization, calculated by projection on all bound states. The sticking occurs mainly between 150 and 400 fs, so that the final sticking probability is obtained after only 450 fs propagation time. Alternatively, one could wait until the reflected parts are absorbed by a complex absorbing potential. However, this would require a much longer propagation time because the reduced probability density has not yet well split into a trapped and a reflected part, after 450 fs (see lower panel).

For the same temperature of 300 K, Fig. 2 shows the convergence of the sticking probability as a function of the iteration number. The difference between consecutive realizations after 60 realizations is about a factor of 10 smaller, compared to the first few realizations. In order to achieve another factor of 10 in precision would require 100 times as

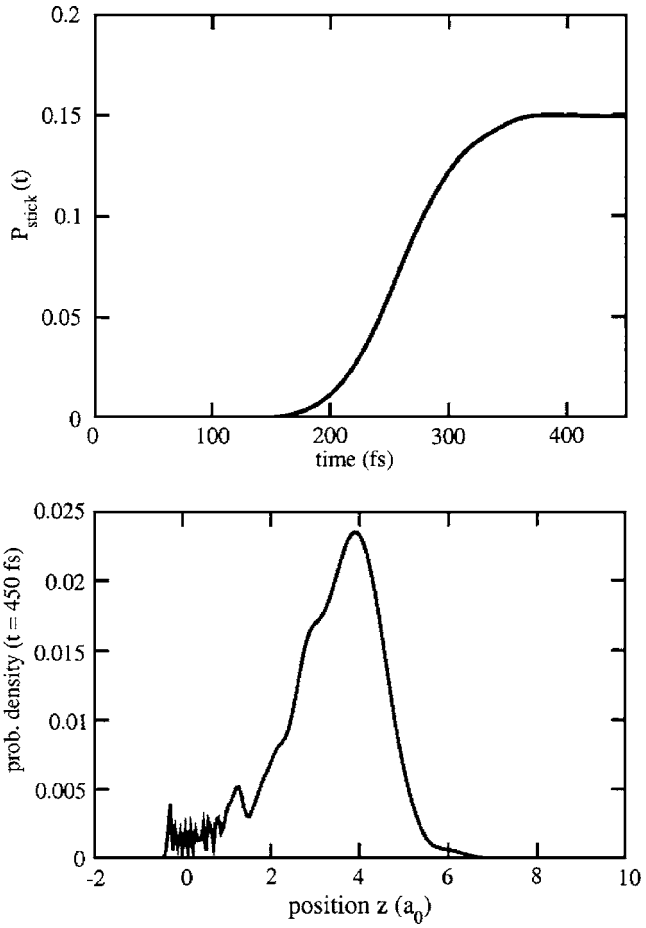

FIG. 1. Upper panel: Exemplary time evolution of the sticking probability, when the scatterer hits a surface at $T=300$ K. Lower panel: Reduced probability density $\rho(z,z',t=450\ \text{fs})$ of the system degree of freedom, at final time $t=450$ fs. Note that the reflected part of the wave packet is not yet clearly separated from the trapped part.

many realizations because our scheme, as any Monte-Carlo scheme, converges with the square root of the number of realizations.

Figure 3 shows histograms for the sticking probabilities

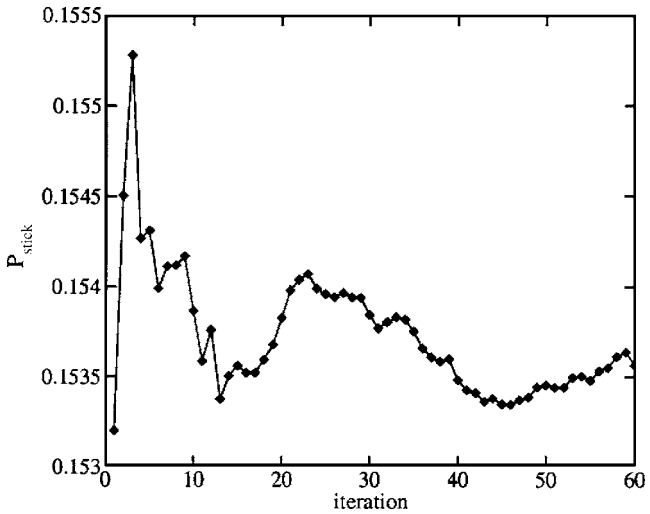

FIG. 2. Convergence of the sticking probability with the number of realizations of the stochastic phase thermal wave function approach, for a surface at $T=300$ K.

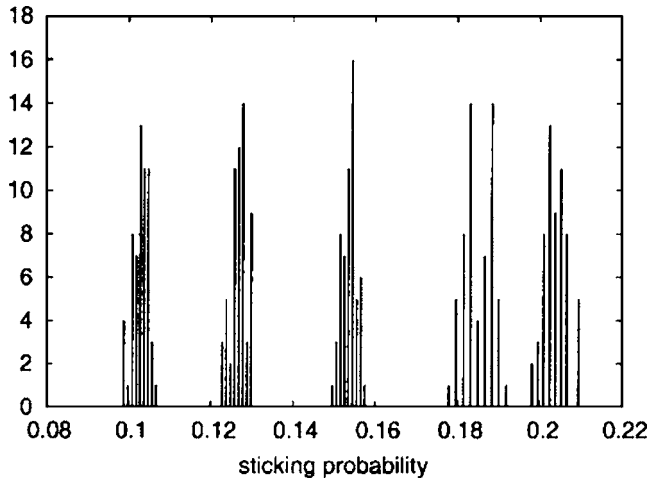

FIG. 3. Histograms of sticking probabilities, for surface temperature of 500, 400, 300, 200, and 100 K, from left to right. For each temperature 60 wave functions were propagated.

for five different temperatures: 500, 400, 300, 200, and 100 K, from left to right. The lowest temperature that we used, 4 K, has been omitted because the bath is practically in a pure state, and the histogram would have only a single line. The large width of the 100 K histogram is rather surprising because the total (i.e., average) sticking probability is almost the same as that for the 4 K case [see Fig. 4 (solid line)]. This implies that for some realizations of the bath at 100 K, the sticking probability is *higher* than that for the 4 K case. Responsible for this unexpected behavior are the low frequency modes. They absorb very different amounts of energy, depending on their phase when the scattering takes place. The higher frequency modes have several oscillation periods during the 200 fs of the scattering event and are therefore less sensitive to the phase.

Next, we would like to discuss the effect that the hot

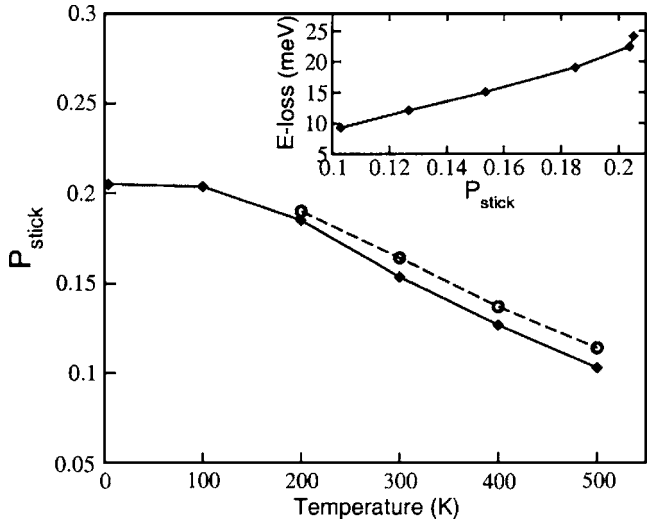

FIG. 4. The main graph shows the sticking probabilities as a function of surface temperature. The solid line with diamonds is the result of our standard configuration of single particle functions. For the dashed line with open circles one more SPF per combined modes has been used. The inset shows how much energy is dissipated from the system, for a given sticking probability.

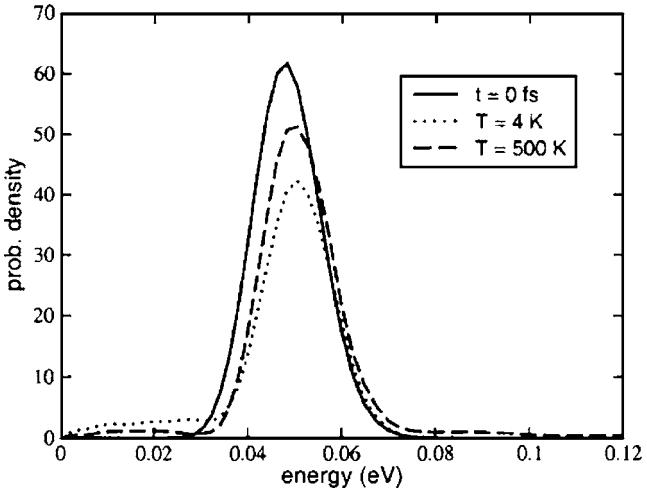

FIG. 5. Kinetic energy density distribution of the scatterer: at the beginning of the propagation (solid line), after reflection from a 4 K surface (dotted line), and from a 500 K surface (dashed line). Only the energy density of the unbound part of the wave packet is shown.

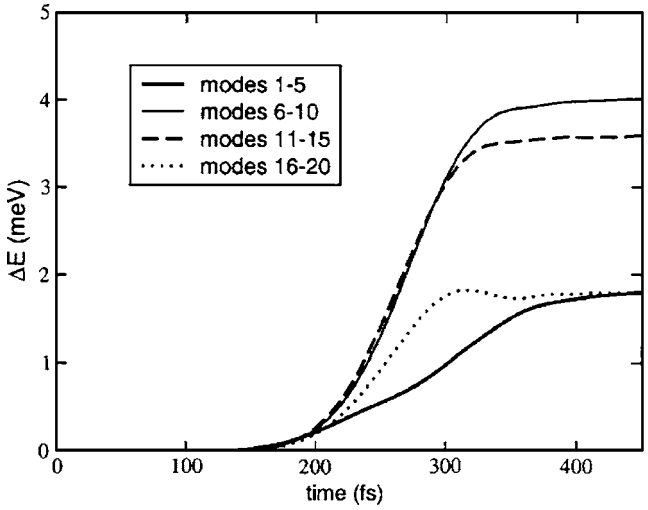

FIG. 6. Energy gain of groups of bath modes. The lowest (thick solid line) and highest (dotted line) frequency modes gained less energy than the medium frequency modes (thin-solid and dashed lines).

surface has on the reflected part of the wave packet. Figure 5 shows the kinetic energy distribution before and after the scattering, for two temperatures. Always only the unbound part of the wave packet is shown. In order to calculate the final kinetic energy distributions, it was necessary to propagate up to 750 fs because the reflected wave packet had to leave the interaction region, in order to be comparable to the incoming wave packet. This is longer than the recurrence time of 608 fs of the bath, but as the scattering starts only at $t=150$ fs, and the contact with the bath is lost after about $t=700$ fs, this is not a serious problem. The solid line in Fig. 5 shows the energy distribution of the incoming wave packet at time $t=0$ fs. By comparison, the areas under the final energy distributions for the reflected wave packets are much smaller. The differences correspond to the sticking probabilities of 20.5% for the dotted line (surface temperature of 4 K) and of 10.3% for the dashed line (surface temperature of 500 K). Also, one can observe that almost all of the adsorbed part of the wave packet originated from the low-energy tail. This indicates a nonlinear increase in the sticking probability with decreasing energy. This has also been found in various other studies before.[34,38] Apart from the main peak, Fig. 5 also shows energy redistribution to lower/higher energies. This is the onset of thermalization, but the average interaction time of ~250 fs is so short, compared to the overall coupling strength parameter of $\gamma=1/(1\ \text{ps})$, that this process has only just begun. At least, it is visible that the 4 K surface transfers more density toward the low-energy regime, while the 500 K surface transfers more density toward the high-energy regime.

Another question one can ask is about the connection between the total amount of dissipated energy and the sticking probability. We find (see inset in Fig. 4) an almost linear relationship between the two: The amount of adsorption is directly proportional to the amount of energy loss of the system. One exception is the very low temperature case, i.e., the range up to 100 K, where a higher energy dissipation does not correlate with a proportionally higher sticking. Tentatively we ascribe this to an increased redistribution of probability density between unbound states. A second deviation from a linear relationship is to be expected for very high temperature cases. Even if the net energy transfer is from the surface to the atom, i.e., for $T>600$ K, it is still conceivable that some part of the wave packet is trapped.

Let us now address the question of where the energy of the scatterer is transferred. We collected the 20 surface modes into four groups and calculated the energy gain over time for them. Figure 6 shows the result for the average over 60 realizations of a 300 K surface. The group with the low frequency surface modes (thick solid line) $x_1,\ldots,x_5$ reacts very slowly to the incoming wave packet and gains only little energy. Most of the energy goes into the medium frequency groups 2 (thin solid line) and 3 (dashed line), which undergo only a small number (2–6) of oscillations during the scattering process. The highest frequency modes (dotted line) $x_{16},\ldots,x_{20}$ gain a similar amount of energy as the lowest frequency modes, but they react faster. One should keep in mind that the coupling coefficients $c_k=k\Delta c$ increase linearly with the number of the bath mode, and that therefore the energy transfer is not only governed by frequency (mis)matching.

The intermediate basis of single particle functions used by the MCTDH ansatz is much smaller than the basis provided by the product of the primitive bases. If the wave function were defined on the product grid, then the representation of a single copy of it would require $\sim 9\times 10^9$ GB of memory and a corresponding amount of CPU time for the propagation. The MCTDH wave function in our standard configuration requires only 3.5 MB of memory and can thus be propagated repeatedly. This configuration is clearly large enough to treat the scattering at low temperatures precisely, but the question arises, up to which temperature such a small basis can reliably represent a thermal wave function. An often used measure for this are the so-called natural populations: For each (combined) degree of freedom the reduced density matrix is calculated and diagonalized. The eigenvalues provide information about the occupation of the SPFs.

The value of the smallest population determines the accuracy of the propagation. Table I gives the maximum of these values during the real time propagation. As a rule of thumb, one can regard a computation as good, if this value is 0.01 or smaller. Thus, especially the low frequency modes have quite high occupations, at high temperature. To check convergence, we added one SPF per combined mode, so that the accuracy of our results can be assessed. Figure 4 shows the new sticking probability with the larger configuration for temperatures from 200 to 500 K. They are higher by 0.5 percentage points at 200 K, and this difference increases up to 1.1 points at 500 K. The latter is about 10% of the total sticking probability, implying that this result is only semiquantitative. In a certain way, this rise of the sticking probability is surprising: If not enough SPFs are used, then the infinite temperature of the bath is not well reproduced, and one ends up at too low an energy after propagation in imaginary time. Because a smaller temperature implies a larger sticking probability, one should expect a decrease, when more SPFs are employed. The fact that we find the opposite indicates some kind of error cancellation. More SPFs also mean a higher amount of correlation, which favors sticking.

IV. SUMMARY

Dynamical simulations of extended quantum systems are extremely difficult due to the exponential computational scaling with the number of DoF. The first reduction in complexity is to concentrate the effort on a system treated explicitly and the rest, the bath, implicitly. If this is done with a reduced density description, then the computational cost is usually very high, and the approximations leading to the dissipative Liouville operator are severe. Wave function descriptions of extended systems require less computational resources. In these formulations which we call surrogate Hamiltonian, the bath is described by a finite number of representative modes which can describe the dynamics adequately up to the recurrence time defined by the bath mode energy spacing. A wave function description defines a pure state; therefore, it would seem that such a description excludes the simulation of mixed states, such as expected at finite temperatures. To overcome this difficulty the random phase thermal wave function method has been introduced.[31,33] In the present paper, it has been developed to simulate the inelastic scattering of an atom at a nonrigid surface at finite temperature.

It is reasonable to expect that the total system-bath system does not develop full quantum correlation, which would still be exponential in the number of degrees of freedom.[8] It has been shown that the environment can limit the growth of quantum correlation or entanglement.[39] These observations can justify calculation methods which are based on limiting the extent of correlations, such as MCTDH. It has a built-in mechanism, which allows us to adjust the wave function to the actual amount of quantum correlations and therefore enables simulations of large systems with moderate computational resources.

In the present paper, we have extended the MCTDH method to incorporate the random phase thermal wave function scheme on the level of the intermediate basis of Hartree products. We have shown that it is sufficient to apply the random phases only on the level of the intermediate basis, i.e., the coefficient tensor A_J. A few dozen realizations were sufficient to converge the algorithm with good accuracy. The typical standard deviation of the sticking probability of about 0.2 percentage points implies an only moderate sensitivity of the sticking probability to the relative phases of the surface oscillators. Additionally, we were able to compute the temperature dependent sticking probability for a wide range of temperatures from 4 to 500 K. The accuracy, which is limited for the higher temperatures due to the finite expansion length, has been assessed. The final kinetic energy distributions show a strong nonlinear energy dependence of the sticking probability, and the onset of thermalization of the scatterer is visible. An analysis of the energy transfer to the bath shows that the cutoff frequency of the surface, and thus its reaction time, was sufficient, so that higher frequencies will not change the sticking probability. However, it is not essential for the general scheme to make this choice. In the simulation of a real system, the cutoff frequency would of course be taken from *ab initio* information.

ACKNOWLEDGMENTS

The authors thank the Deutsche Forschungsgemeinschaft for financial support through project SfB 450 and the Israel Science Foundation. One of us (M.N.) also thanks the Fritz-Haber-Center of the Hebrew University Jerusalem for its hospitality.

[1] H.-P. Breuer and F. Petruccione, *The Theory of Open Quantum Systems* (Oxford University Press, Oxford, 2002).
[2] V. May and V. Kühn, *Charge and Energy Transfer Dynamics in Molecular Systems* (Wiley-VCH, Berlin, 2000).
[3] P. P. Saalfrank, M. Nest, I. Andrianov, T. Klamroth, D. Kröner, and S. Beyvers, J. Phys.: Condens. Matter **19**, 1425 (2006).
[4] S. Dittrich, H.-J. Freund, C. P. Koch, R. Kosloff, and T. Klüner, J. Chem. Phys. **124**, 024702 (2006).
[5] S. Lee and J. T. Hynes, J. Chem. Phys. **88**, 6853 (1988).
[6] M. Thorwart, M. Grifoni, and P. Hänggi, Phys. Rev. Lett. **85**, 860 (2000).
[7] P. Hyafil, J. Mozley, A. Perrin, J. Tailleur, G. Nogues, M. Brune, J. M. Raimond, and S. Haroche, Phys. Rev. Lett. **93**, 103001 (2004).
[8] *Decoherence and the Appearance of a Classical World in Quantum Theory*, edited by D. Giulini, E. Joos, C. Kiefer, J. Kupsch, I. O. Stamatescu, and H. D. Zeh (Springer, Berlin, 2003).
[9] F. Haake, H. Risken, C. Savage, and D. Walls, Phys. Rev. A **34**, 3969 (1986).
[10] R. Alicki and K. Lendi, *Quantum Dynamical Semigroups and Applications*, Springer Lecture Notes in Physics Vol. 286 (Springer, Berlin, 1987).
[11] A. G. Redfield, Phys. Rev. **98**, 1787 (1955).
[12] A. G. Redfield, IBM J. Res. Dev. **1**, 19 (1957).
[13] A. O. Caldeira and A. J. Leggett, Phys. Rev. A **31**, 1059 (1985).
[14] M. Thoss and W. Domcke, J. Chem. Phys. **109**, 6577 (1998).
[15] W. T. Pollard and R. A. Friesner, J. Chem. Phys. **100**, 5054 (2001).
[16] G. Lindblad, Commun. Math. Phys. **48**, 119 (1976).
[17] C. Meier and D. J. Tannor, J. Chem. Phys. **111**, 3365 (1999).
[18] E. Geva, R. Kosloff, and J. L. Skinner, J. Chem. Phys. **102**, 8541 (1995).
[19] M. Berman, R. Kosloff, and H. Tal-Ezer, J. Phys. A **25**, 1283 (1992).
[20] P. Saalfrank, R. Baer, and R. Kosloff, Chem. Phys. Lett. **230**, 463 (1994).
[21] W. Huisinga, L. Pesce, R. Kosloff, and P. Saalfrank, J. Chem. Phys. **110**, 5538 (1999).
[22] R. Baer and R. Kosloff, J. Chem. Phys. **106**, 8862 (1997).
[23] N. V. Prokof'ev and P. Stamp, Rep. Prog. Phys. **63**, 669 (2000).
[24] S. Tsonchev and P. Pechukas, Phys. Rev. E **61**, 6171 (1999).
[25] H.-D. Meyer, U. Manthe, and L. S. Cederbaum, Chem. Phys. Lett. **165**,

73 (1990).
[26] M. H. Beck, A. Jäckle, G. A. Worth, and H.-D. Meyer, Phys. Rep. **324**, 1 (2000).
[27] H.-D. Meyer and G. A. Worth, Theor. Chem. Acc. **109**, 251 (2003).
[28] H. Wang and M. Thoss, J. Chem. Phys. **119**, 1289 (2003).
[29] H. Wang and M. Thoss, J. Chem. Phys. **124**, 034114 (2006).
[30] R. Martinazzo, M. Nest, P. Saalfrank, and G. F. Tantardini, J. Chem. Phys. **125**, 194102 (2006).
[31] U. Manthe and F. Huarte-Larrañaga, Chem. Phys. Lett. **349**, 321 (2001).
[32] U. Manthe, G. Capecchi, and H.-.J. Werner, Phys. Chem. Chem. Phys. **6**, 5026 (2004).
[33] D. Gelman and R. Kosloff, Chem. Phys. Lett. **381**, 129 (2003).
[34] M. Nest and H.-D. Meyer, J. Chem. Phys. **119**, 24 (2003).
[35] D. Gelman, C. P. Koch, and R. Kosloff, J. Chem. Phys. **121**, 661 (2004).
[36] M. Nest and P. Saalfrank, J. Chem. Phys. **116**, 7189 (2002).
[37] H.-D. Meyer, The MCTDH Package, Version 8.3 (2002), see http://www.pci.uni-heidelberg.de/tc/usr/mctdh/
[38] M. Nest and P. Saalfrank, J. Chem. Phys. **113**, 8753 (2000).
[39] M. Khasin and R. Kosloff, Phys. Rev. A **76**, 012304 (2007).